Synthesis and Characterization of Polyvinylferrocene/Polypyrrole Composites

Songül Şen[a]; Ayşegül Uygun Gök[b]; Handan Gülce[c]; Matt Aldissi[d]
[a] Faculty of Arts and Sciences, Department of Chemistry, Mehmet Akif Ersoy University, Burdur, Turkey [b] Faculty of Arts and Sciences, Department of Chemistry, Süleyman Demirel University, Isparta, Turkey [c] Faculty of Engineering and Architecture, Department of Chemical Engineering, Selçuk University, Konya, Turkey [d] Fractal Systems, Inc., Safety Harbor, FL, USA

PLEASE SCROLL DOWN FOR ARTICLE

Synthesis and Characterization of Polyvinylferrocene/ Polypyrrole Composites

SONGÜL ŞEN,[1] AYŞEGÜL UYGUN GÖK,[2] HANDAN GÜLCE,[3] and MATT ALDISSI[4]

[1]*Faculty of Arts and Sciences, Department of Chemistry, Mehmet Akif Ersoy University, Burdur, Turkey*
[2]*Faculty of Arts and Sciences, Department of Chemistry, Süleyman Demirel University, Isparta, Turkey*
[3]*Faculty of Engineering and Architecture, Department of Chemical Engineering, Selçuk University, Konya, Turkey*
[4]*Fractal Systems, Inc. Safety Harbor, FL, USA*

Conducting polymer composites of polyvinylferrocene and polypyrrole (PVF/PPy) were synthesized chemically by the *in situ* polymerization of pyrrole in the presence of PVF using FeCl$_3$ as oxidant. Acetic (CH$_3$COOH) and boric (H$_3$BO$_3$) acids were used as the synthesis medium. Effects of the synthesis medium on the properties of the PVF/PPy composite were investigated. The PVF/PPy composites and homopolymers were characterized by fourier transform infrared spectroscopy (FTIR), thermogravimetric analysis (TGA), scanning electron microscopy (SEM), energy dispersive spectroscopy (EDS) and magnetic susceptibility techniques. Conductivity measurements were performed using the four-probe technique. We found that the conductivities of PVF/PPy-H$_3$BO$_3$ (1.19 S cm^{-1}) and PVF/PPy-CH$_3$COOH (4.5×10^{-1} S cm^{-1}) increased relative to those of the homopolymers of PPy-H$_3$BO$_3$ (2.1×10^{-2} S cm^{-1}) and PPy-CH$_3$COOH (1.2×10^{-2} S cm^{-1}) due to the interaction of PVF with the pyrrole moiety. The stability of all homopolymers and composites were investigated by thermogravimetric analysis and by conductivity measurements during heating-cooling cycles. There was a small drop in conductivity caused by the annealing of PVF/PPy composites at 70°C. The conductivity of all samples increased with temperature and exhibited stable electrical behavior with increasing temperature. TGA analysis of samples showed that the composites were more stable than the homopolymers or PVF separately. The magnetic susceptibility values of samples were negative, except for PVF/PPy-H$_3$BO$_3$. Morphology changes of the composites investigated by scanning electron microscopy (SEM), attributed to synthesis conditions, have a significant effect on their conductivity.

Keywords: polyvinylferrocene; polypyrrole; composite; conductivity; thermal stability

1 Introduction

Intrinsically conducting polymers (ICPs) such as PPy have been widely investigated with a view to improving their processibility, and physical and chemical properties (1, 2). During the last two decades, investigations have centered mainly on improvement of the physical properties of PPy such as processibility and stability. PPy has been identified for certain specific applications such as rechargeable batteries (3), conducting textiles (4) and as membranes for gas separation processes (5, 6), non-linear optical devices (7), light emitting diodes (8), electrochemical sensors (9), molecular magnets (10), thin film transistors (11) and catalysts for chemical reactions. Improvements are expected from composite materials where the conducting polymer exhibits the desired conductivity, while the composite matrix provides the needed mechanical properties. Namely, a combination of two polymer matrices allows the creation of new polymeric materials with interesting electrical and mechanical properties (12–15). The mechanical properties can be enhanced by forming composites from a conductive polymer and a conventional insulating polymer (16). To improve the structural and electrical properties of the composite materials, samples containing ICPs like PPy and non-conducting materials like poly (vinyl chloride) (17), poly (vinyl alcohol) (18), polyurethane (19), and polycarbonate (20) or poly (ethylene-vinyl alcohol) (21) were synthesized.

One type of conductive composites consists of combining ICPs with organometallic materials, such as ferrocene (Figure 1) which is the subject of this study. Combining the properties of electroactive polymers with those of metallocene is a very exciting challenge. The redox polymer poly (vinylferrocenium) perchlorate (PVF$^+$ClO$_4^-$) gives rise to some interesting electrochemical results when used as a

Address correspondence to: Songül Şen, Faculty of Arts and Sciences, Department of Chemistry, Mehmet Akif Ersoy University, Burdur 15100, Turkey. Fax: +90-2482122718; E-mail: ssen@ mehmetakif.edu.tr
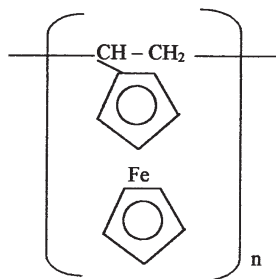
Fig. 1. Molecular structure of PVF (8).

layer on Pt surfaces. This electroative film can act as a modified surface through which an electron transfer between a substrate and a reactant can take place. Studies related to the reduction and oxidation of some reactants through this film have been reported (22, 23). PVF is used in this study as an insulating matrix in the synthesis of PPy composite for the first time to the best of the author's knowledge.

The aim of the present study was to develop enhanced physical properties such as electrical and thermal stability of PPy using PVF homopolymer. Additionally, the effect of synthesis media on the properties of PVF/PPy composites was investigated using boric and acetic acids showing different pKa values. For comparison, PPy homopolymer was synthesized in the same acidic conditions. The prepared composites were characterized by SEM, FTIR and EDS measurements. The stability of PVF/PPy composites was investigated by thermogravimetric analysis. Conductivity was measured during heating-cooling cycles and the isothermal stability of composites was carried out at 70, 85 and 100°C.

2 Experimental

Ferric chloride, $FeCl_3$, (Riedel de Haen) was used as an oxidizing agent for chemical polymerization of pyrrole (Figure 2) (Merck). The acidic media were prepared using H_3BO_3 (pKa = 5.9×10^{-10}) and CH_3COOH (pKa = 1.8×10^{-5}) (Merck). PVF was prepared by chemical polymerization of its monomer, vinylferrocene (Aldrich), by 2,2′-Azobis (2-methylbutyronitrile) (Acros Organics) at 70°C (24).

For the synthesis of PVF/PPy composite, 0.03 g PVF in 100 mL acid solution was shaken for 15 min in an ultrasonic bath which resulted in a good dispersion of PVF. Then, 10 mmol pyrrole was added to this dispersion and shaking continued for 15 min in the ultrasonic bath. The
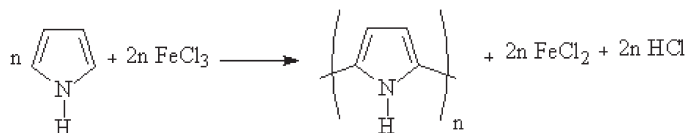

Fig. 2. Oxidation polymerization process of pyrrole by $FeCl_3$.

polymerization of pyrrole was initiated by the dropwise addition of the oxidizing agent ($FeCl_3$, 25 mmol) in 1 M acids solution (H_3BO_3 and CH_3COOH) under constant stirring at 0–5°C. The ratio of oxidizing agent to monomer was 2.5. After complete addition of the oxidizing agent, the reaction mixture was kept under constant stirring for 16 h. The precipitated composite was filtered and washed with acid solution first, then washed with distilled water until the filtrate was colorless. Finally, the polymer was dried at 50°C for 24 h under vacuum. Composition of PVF/PPy composite was described as (4.3/95.7) in (w/w, %) for both two synthesis media. PPy homopolymer was synthesized in the same conditions using both synthesis media (H_3BO_3 and CH_3COOH) and purified in a similar manner.

Scanning electron microscopy (SEM) and EDS (energy dispersive spectroscopy) analysis of the polymers were performed using JEOL.JEM 100CX model scanning electron microscope. FTIR spectra were recorded on a Perkin-Elmer model spectrometer. Thermograms were recorded by using a Perkin-Elmer thermogravimetric analyzer in the presence of N_2 atmosphere from 25 to 900°C at a heating rate of 10°C min^{-1}. The direct current electrical conductivity of samples was measured by a standard four-probe method. Current (I), potential (V) and temperature (t) were controlled using PCI-DAS6014 card. Dry powdered samples were made into pellets using a steel die having 13 mm diameter in a hydraulic press under a pressure of 200 MPa. Temperature dependent electrical conductivity of the polymer samples was measured by four probe system with PCI-DAS6014 connected to computer and, the temperature of pellets was recorded with a thermocouple. The dependence of electrical conductivity of the composite was measured over a temperature range from 25 to 70, 85 and 100°C. Electrical properties of composites were investigated between 25–100°C with heating-cooling cycles and, thermal aging studies were made at 70, 85, and 100°C. Magnetic susceptibility measurements were taken on a Sherwood Scientific model Gouy balance using a pyrex glass capillary tube filled with the sample.

3 Results and Discussion

3.1 FTIR Results

The infrared spectra of samples prepared with different organic acids were taken in the region from 4000 to 400 cm^{-1} (Figure 3a–b). The band at 1532 cm^{-1} in the spectrum of PPy-CH_3COOH (Figure 3a) corresponds to the C-C strectching vibrations in the pyrrole ring. This band has been observed at 1534 cm^{-1} for PPy- H_3BO_3 (Figure 3b). The PPy-H_3BO_3 bands are sharper than those of PPy-CH_3COOH. It is known that the skeletal vibrations, involving the delocalized π-electrons, are affected by doping of the polymer (25). The band at 1448 cm^{-1} in the spectra of homopolymers corresponds to C-N stretching
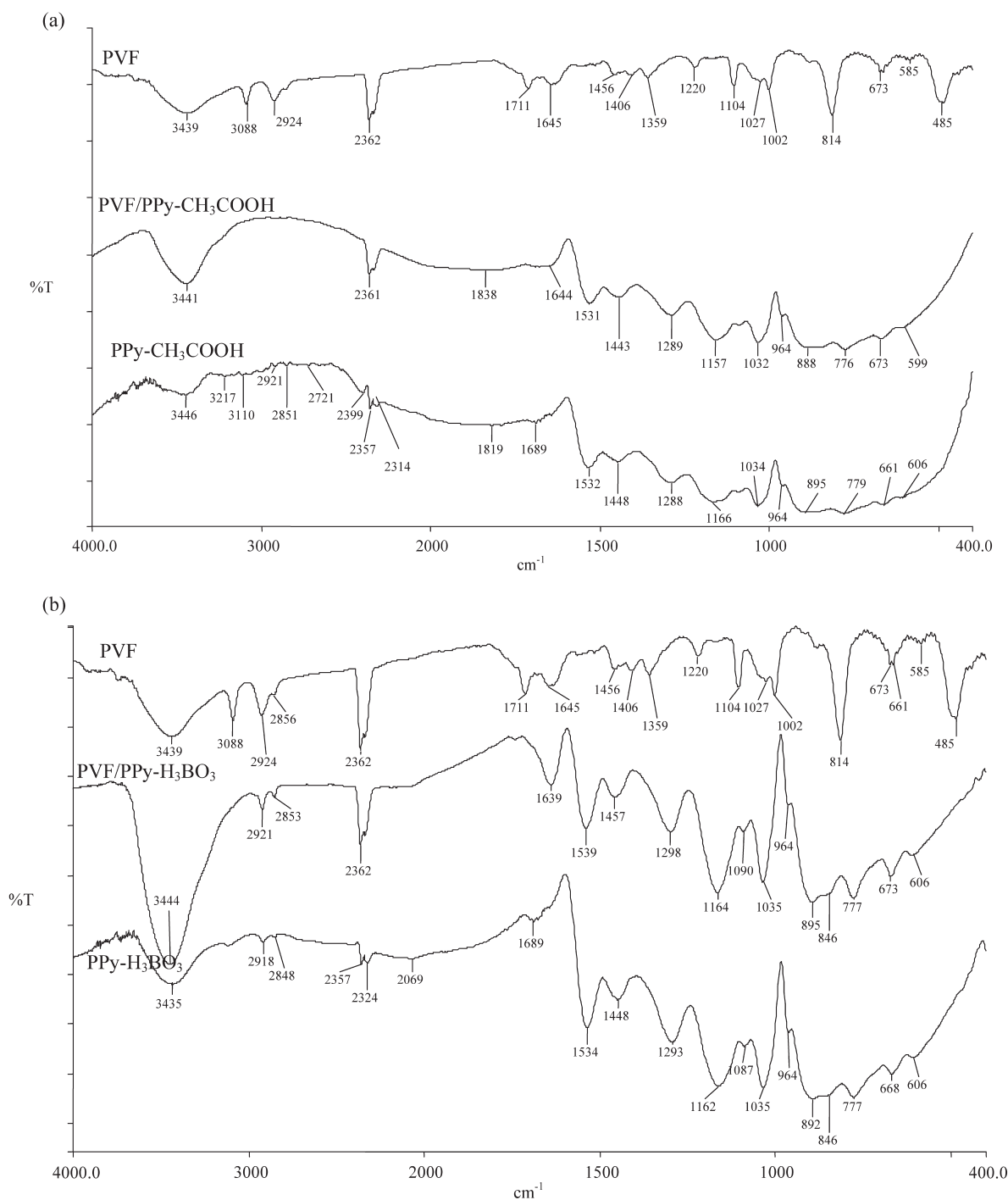
Fig. 3. FTIR spectra of samples synthesized in (a) acetic acid and (b) boric acid medium.

vibration in the ring. The band at 1289 cm^{-1} in the spectrum of PPy-CH$_3$COOH is attributed to C-H or C-N in-plane deformation modes. This band shifted to 1293 cm^{-1} for PPy-H$_3$BO$_3$. The difference in the spectra of PPy-CH$_3$COOH and PPy-H$_3$BO$_3$ samples was also found at the 1166 and 1162 cm^{-1} bands, respectively, which is attributed to the breathing vibration of the pyrrole ring.

The band at 1035 cm^{-1}, which corresponds to C-H and N-H in-plane deformation vibration, is present in both homo-polymers. The band at 964 cm^{-1}, which is attributed to C-C out-of-plane ring deformation vibration, is situated at the same position in the spectra of both samples. The band of C-H out of plane deformation vibrations of the ring has a maximum at 779 cm^{-1} for PPy-CH$_3$COOH and at 777 cm^{-1} for PPy-H$_3$BO$_3$. All these peaks can be observed

well in the PVF/PPy-CH$_3$COOH and PVF/PPy-H$_3$BO$_3$ composites. These results indicate that the structure of the polypyrrole backbone in PVF/PPy-CH$_3$COOH and PVF/PPy-H$_3$BO$_3$ composites is similar to that of PPy-CH$_3$COOH and PPy-H$_3$BO$_3$ homopolymers, respectively.

In the infrared spectra of PVF, the band of C-H stretching vibrations of PVF has a maximum at 3088 cm^{-1}. The bands at 1002 and 1406 cm^{-1} correspond to the C-H out-of-plane

bending vibrations. The band at 1104 cm^{-1} in the spectra of PVF is attributed to C-C stretching modes. The band at 814 cm^{-1} in the spectra of PVF is shifted to higher wavenumbers, which were at 888 cm^{-1} and 895 cm^{-1} for PVF/PPy-CH$_3$COO and PVF/PPy-H$_3$BO$_3$, respectively.

A qualitative method to obtain a relative measure of the conjugation length of PPy from FTIR measurements, which is based on a parameter called the "effective conjugation
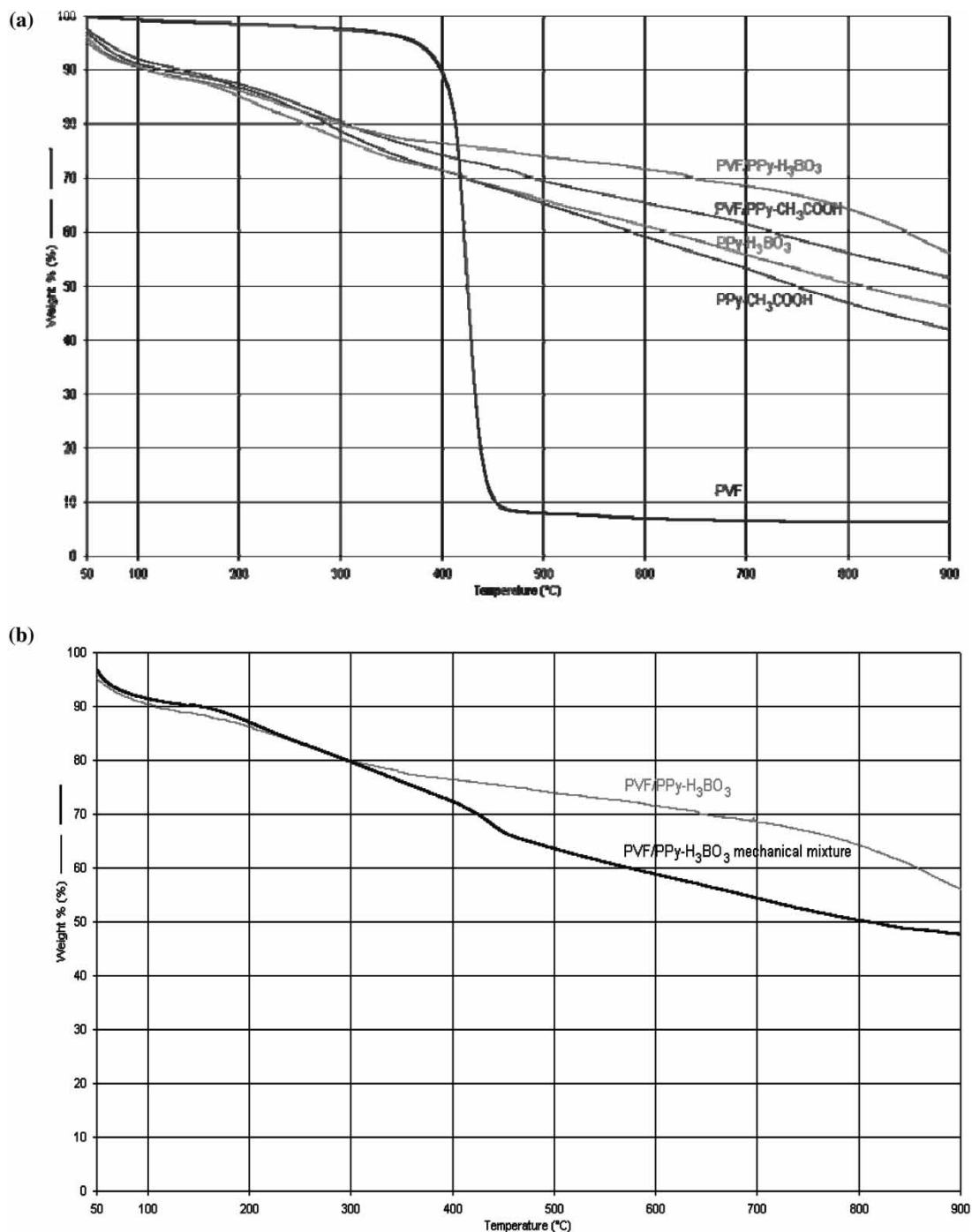

Fig. 4. TGA analysis of (a) all samples and (b) comparison of PVF/ PPy-H$_3$BO$_3$ and PVF/PPy-H$_3$BO$_3$ mechanical mixture.

coordinate" was found by Menon et al. (26). This was an extension of work by Tian and Zerbi (27) where they demonstrate by theoretical calculations that as the conjugation length increases, the intensity of the antisymmetric ring stretching mode at 1535 cm^{-1} (A_{1535}) decreases and the intensity of the symmetric mode at 1445 cm^{-1} (A_{1445}) increases. When we compare the spectra of PPy-H$_3$BO$_3$ and PVF/PPy-H$_3$BO$_3$, the band at 1534 cm^{-1} in the spectrum of PPy-H$_3$BO$_3$ has shifted to 1539 cm^{-1} in the spectrum of the composite without a change in intensity. The band at 1448 cm^{-1} in the spectrum of PPy-CH$_3$COOH and PPy-H$_3$BO$_3$ has shifted to 1443 and 1457 cm^{-1} for PVF/PPy-CH$_3$COOH and PVF/PPy-H$_3$BO$_3$, respectively. The intensity of this band has increased slightly in the spectrum of PVF/PPy-CH$_3$COOH relative to that of the homopolymer. These results show that the conjugation of PVF/PPy-CH$_3$COOH is better than its homopolymer counterpart.

3.2 TGA Results

Figure 4a shows the TGA curves of the different samples. The low weight loss (8%) observed in the range of 70−100°C is due to moisture being removed from PPy (28) and PVF/PPy samples. Thermal degradation temperatures and residue % at 900°C obtained from these curves are shown in Table 1.

Pure PVF shows one step weight loss in the temperature range of 410−435°C. The weight loss is nearly 94%. PPy-H$_3$BO$_3$, and PVF/PPy-H$_3$BO$_3$ demonstrate a one-step weight loss as well, except for the low mass loss at 85°C due to moisture. A sharp weight loss appears in the temperature range of 167−345°C for PPy-H$_3$BO$_3$ and 190−290°C for PVF/PPy-H$_3$BO$_3$, which is related to removel of dopant anion and thermal decomposition of the polymer chains (29). PPy-CH$_3$COOH and PVF/PPy-CH$_3$COOH show a two-step weight loss. For the PPy-CH$_3$COOH and PVF/PPy-CH$_3$COOH, the first weight losses, in the range of 180−290 and 235−305°C, respectively, indicate removing dopant anions from polymer structure. The second weight

loss step for the same samples, which are in the temperature range of 590−850 and 672−810°C, respectively, is related to thermal decomposition of the polymer chains. Apparently, the PVF/PPy composite exhibits better thermal stability than the PPys and PVF separately. The decomposition temperature of PPy-H$_3$BO$_3$ increased from 167 to 190°C and the decomposition temperature of PPy-CH$_3$COOH increased from 180 to 235°C when their composites were prepared with PVF.

Furthermore, the composites are more stable than their homopolymer counterparts. The weight losses of PPy-H$_3$BO$_3$ and PPy-CH$_3$COOH were 53 and 58%, while the weight losses of PVF/PPy-H$_3$BO$_3$ and PVF/PPy-CH$_3$COOH were 44 and 49%, respectively. However, the trend of the degradation curves of the composites is similar to that of the homopolymers; the degradation of the composite is mainly controlled by the homopolymer. At the same time, the thermal stability of composites is higher than that of PVF.

Additionally, we prepared the PVF:PPy-H$_3$BO$_3$ mixture mechanically using the same composition to understand whether the composite is a simple mixture or not. TGA results of PVF:PPy-H$_3$BO$_3$ mixture exhibited a two-step decomposition showing both initial decomposition temperatures of PVF and PPy-H$_3$BO$_3$ (Figure 4b). Moreover, PVF/PPy-H$_3$BO$_3$ composite has different decomposition behaviour from PVF:PPy-H$_3$BO$_3$ mechanical mixture. These results may indicate that the composites prepared *in-situ* polymerization are not simple mixtures of PVF and PPy homopolymers.

3.3 SEM Studies of Samples

SEM images of homopolymers, PVF and composites are given in Figure 5(a−e). PPy-CH$_3$COOH (Figure 5a) has a globular morphology compared to PPy-H$_3$BO$_3$ (Figure 5b). PPy-H$_3$BO$_3$ has more flat and "leafy" morphology. The size of PVF particles (Figure 5c) is higher than those of the PPy homopolymers and composites. PVF/PPy-CH$_3$COOH composite (Figure 5d) looks more compact than PVF/PPy-H$_3$BO$_3$ (Figure 5e). The SEM study of PVF/

Table 1. Thermal degradation temperatures of samples

Sample	Synthesis medium	T_i (°C)	T_m (°C)	T_f (°C)	Residue % at 1000°C
PVF	Benzene	410	422.5	435	6.2
PPy-H$_3$BO$_3$	1 M H$_3$BO$_3$	167	256	345	47
PVF/PPy-H$_3$BO$_3$	1M H$_3$BO$_3$	190	240	290	56
PVF/PPy-H$_3$BO$_3$ mechanical mixture	−	168	289	410	47
		410	427.5	445	
PPy-CH$_3$COOH	1 M CH$_3$COOH	180	235	290	42
		590	720	850	
PVF/PPy-CH$_3$COOH	1M CH$_3$COOH	235	270	305	51
		672	741	810	

T_i: Initial decomposition temperature.
T_m: Maximum decomposition temperature.
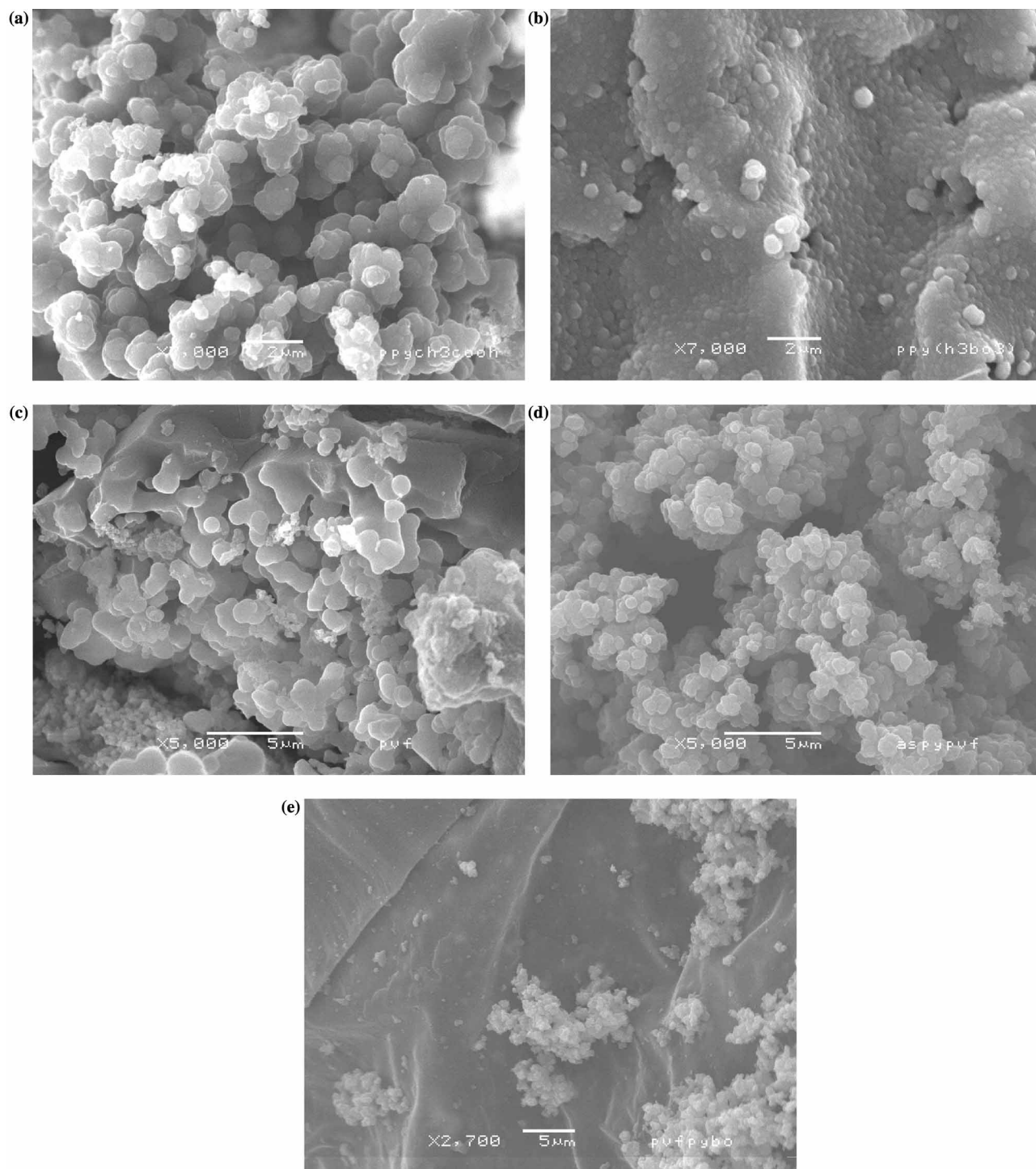T_f: Final decomposition temperature.

Fig. 5. SEM images of (a) PPy-CH$_3$COOH, (b) PPy-H$_3$BO$_3$, (c) PVF, (d) PVF/PPy-CH$_3$COOH, (e) PVF/PPy-H$_3$BO$_3$.

PPy-CH$_3$COOH (Figure 5d) sample reveals the presence of globular particles of less than that of PVF and the particles create agglomerates, also. The SEM micrograph of PVF/PPy-H$_3$BO$_3$ (Figure 5e) shows a flat image. The appearance of the surface of PVF/PPy-H$_3$BO$_3$ particles as they are formed in the polymerization media changes from rougher to smoother surfaces. As shown by SEM, the original

structure of the untreated PVF (Figure 5c) changed after being covered with PPy (Figure 5d and e).

3.4 Conductivity Results

Figure 6(a–d) shows the conductivity versus temperature curves of PPys and PVF/PPy composites synthesized in
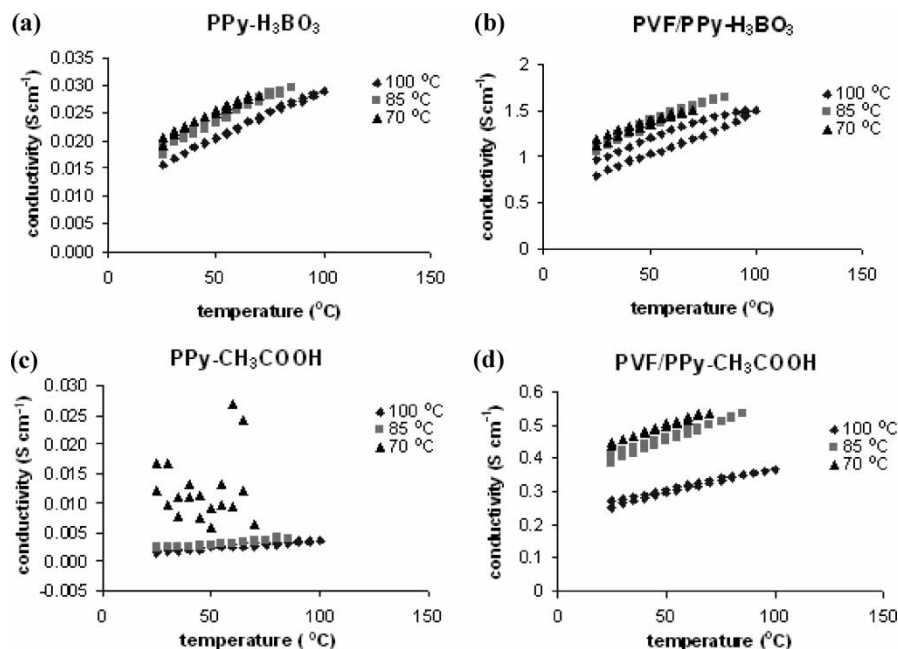
Fig. 6. Temperature dependent conductivity plots of samples doped with different acids (a) PPy-H$_3$BO$_3$, (b) PVF/PPy-H$_3$BO$_3$, (c) PPy-CH$_3$COOH, (d) PVF/PPy-CH$_3$COOH.

different acidic media. The increase in conductivity with increasing temperature is characteristic of the "thermal activated behavior" of ICPs in general (30). This thermal activation results from the increase of efficiency of charge transfer between the polymer chains and the dopant ions (31). Also, there can be thermal curing, which affects the chain alingment of the polymer and leads to the increase of the conjugation length and that brings about the increase of conductivity. There also can be molecular rearrangement on heating, which made the molecular conformation favourable for electron delocalization (32). As seen from Figure 6c, PPy-CH$_3$COOH is not stable in the range of 25−70°C or in the other ranges. In contrast, the PVF/PPy-CH$_3$COOH composite showed more stable and conductive material than PPy-CH$_3$COOH.

The conductivity values of samples at 25°C, after finishing every cyclic treatments, were given at Table 2. The conductivity value of untreated PPy-H$_3$BO$_3$ decreased from 2.1×10^{-2} to 1.6×10^{-2} S cm^{-1} in the end of three cycle treatments. The decrease of conductivity for all samples were observed after

the third cyclic treatment. Among all samples, PPy-CH$_3$COOH indicates the highest decrease of conductivity value (∼10 times). It was observed that other samples have quite stable conductivity values after cyclic treatments.

The conductivity results at room temperature (Table 3) show that PVF/PPy-H$_3$BO$_3$ (1.19 S cm^{-1}) and PVF/PPy-CH$_3$COOH (4.5×10^{-1} S cm^{-1}) composites are more conductive than PPy-H$_3$BO$_3$ (2.1×10^{-2} S cm^{-1}) and (PPy-CH$_3$COOH) (1.2×10^{-2} S cm^{-1}). The conductivity value of PVF:PPy-H$_3$BO$_3$ mixture is however similar to pure PPy-H$_3$BO$_3$. This result also confirmed the PVF/PPy composites are not simple mixtures.

There are strong interactions between PVF and PPy in the composites. PVF/PPy-H$_3$BO$_3$ and PVF/PPy-CH$_3$COOH composites have different conductivity values showing the effect of the synthesis acidic medium. The pKa value of H$_3$BO$_3$ is lower than that of CH$_3$COOH. The medium acidity affected the properties of the composites as well as their homopolymers. We measured conductivities of PPy synthesized in the presence of different media (without acid, inorganic acids and organic acids). The detailed results of this study will be published separately. According to their conductivity results, the best conductivity values among these synthesis media were obtained in the presence of H$_3$BO$_3$ and CH$_3$COOH, which prompted us to prepare the PVF/PPy composites using these acids.

The conductivity values of composites increased with evaluating temperature. All samples exhibited stable electrical behavior with increasing temperature in the heating-cooling cycles. All of the samples followed the Arrhenius equation for temperature dependence of electrical conductivity, as shown in Figure 7(a−d). This suggests the semi-conducting

Table 2. Conductivity values of samples at room temperature after cyclic treatments

Sample σ (S cm^{-1})	PPy-H$_3$BO$_3$	PVF/PPy-H$_3$BO$_3$	PPy-CH$_3$COOH	PVF/PPy-CH$_3$COOH
Untreated	2.1×10^{-2}	1.194	1.2×10^{-2}	4.5×10^{-1}
After cycle 1	1.9×10^{-2}	1.118	1.6×10^{-2}	4.4×10^{-1}
After cycle 2	1.7×10^{-2}	1.137	2.2×10^{-3}	3.9×10^{-1}
After cycle 3	1.6×10^{-2}	0.796	1.6×10^{-3}	2.5×10^{-1}

Cycle 1: 25−70°C, cycle 2: 25−85°C, cycle 3: 25−100°C.

Table 3. Conductivity and mass magnetic susceptibility measurements of samples

Polymer	Synthesis media	Conductivity at 25°C (S cm^{-1})	Mass magnetic susceptibility (χg)
PVF	Benzene	–	-1.3×10^{-6}
PPy-H$_3$BO$_3$	1 M H$_3$BO$_3$	2.1×10^{-2}	-1.5×10^{-6}
PVF/PPy-H$_3$BO$_3$	1 M H$_3$BO$_3$	1.194	2.37×10^{-5}
PVF/PPy-H$_3$BO$_3$ mechanical mixture	–	2.5×10^{-2}	–
PPy-CH$_3$COOH	1 M CH$_3$COOH	1.2×10^{-2}	-2.3×10^{-6}
PVF/PPy-CH$_3$COOH	1 M CH$_3$COOH	4.5×10^{-1}	-2.23×10^{-6}

nature of the samples. The PPy-CH$_3$COOH deviated from the Arrhenius equation on and off until 65°C. After this temperature conductivity followed the Arrhenius equation.

The stability of electrical conductivity of the samples was studied under isothermal conditions at 70, 85, 100°C. The temperature of the composites was maintained at the temperature of study, and the conductivity (σ) was measured every 5 min in an accelerated aging experiment.

The electrical conductivity measured with respect to time of accelerated aging is presented in Figure 8(a–b). For PVF/PPy–H$_3$BO$_3$, the electrical conductivity decreased with time at 70, 85 and 100°C, which was attributed to the loss of the dopant anion. PVF/PPy-H$_3$BO$_3$ lost 35% of its conductivity value after this treatment. For PVF/PPy-CH$_3$COOH, the electrical conductivity first increased during the first 10 min, then it started decreasing slowly with time at 70, 85 and 100°C. This was attributed to the loss of dopant, the chemical reaction of the dopant with the polymer, and the semiconductor-to-metal transition.

PVF/PPy-CH$_3$COOH lost only 10% of its conductivity value. Thus, these measurements showed that PVF/PPy-CH$_3$COOH is more stable than PVF/PPy-H$_3$BO$_3$ in this accelerated aging process, which confirms the thermogravimetric analysis results.

3.5 Magnetic Susceptibility Results

Table 3 shows the mass magnetic susceptibility measurements of composites and homopolymers. As seen in Table 3, the mass magnetic susceptibility value of PVF/PPy- H$_3$BO$_3$ is positive, whereas the other polymers are negative. Negative magnetic susceptibility values reveal diamagnetism and positive values demonstrate paramagnetism (33). These analyses indicate that the conduction mechanism of PVF/PPy-H$_3$BO$_3$ is polaronic by nature (Figure 9a), whereas conductivity of the other polymers is due to bipolarons (Figure 9b) (34).
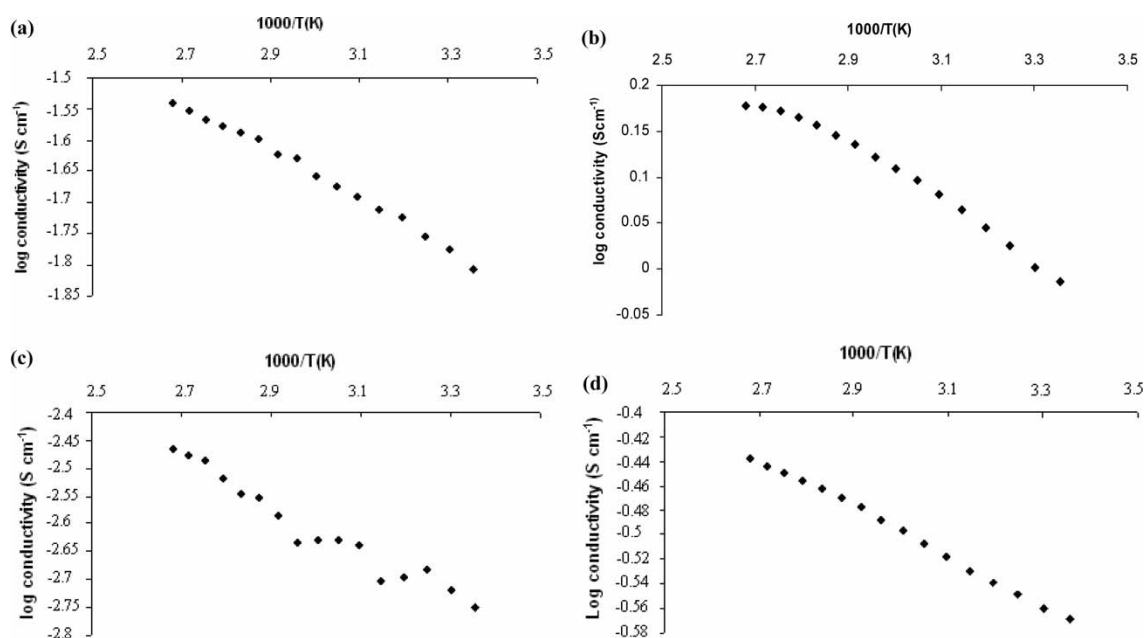
Fig. 7. The effect of temperature on conductivity PPy-H$_3$BO$_3$ (a), PVF/PPy-H$_3$BO$_3$ (b), PPy-CH$_3$COOH (c), PVF/PPy-CH$_3$COOH (d).
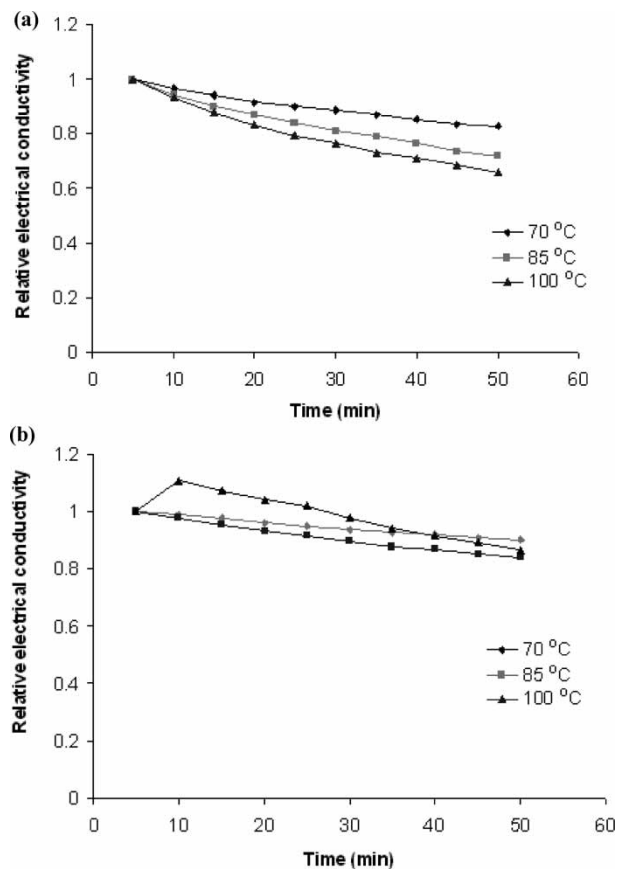
Fig. 8 Isothermal stability of (a) PVF/PPy-H_3BO_3 and (b) PVF/PPy-CH_3COOH composites in terms of retention of σ with respect to time at 70, 85 and 100°C.
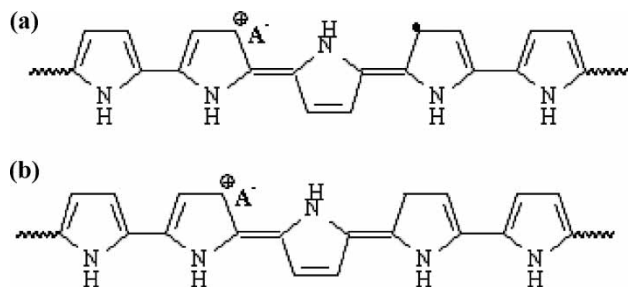

Fig. 9 Polaron (a) and bipolaron (b) structures of polypyrrole.

4 Conclusions

Conducting PVF/PPy composites were prepared in the presence of H_3BO_3 and CH_3COOH acids. PPy homopolymers and PVF/PPy composites indicated different properties as depending on synthesis media. The chemical oxidative modification of polypyrrole by PVF enables the fabrication of composites with conductivity in the range of 1.194–4.5×10^{-1} S cm^{-1}, which is higher than that of their homopolymer counterparts. The PVF/PPy composites have better thermal stability and conductivity values than those of PPy homopolymers. The preparation of these composites may find some applications in the biosensor systems. The biosensor activity of the prepared composites are under consideration in our group.

5 Acknowledgments

6 References

1. Mravcakova, M., Boukerma, K., Omastova, M. and Chehimi, M.M. (2006) *Materials Sci. and Eng., C.*, **26**, 306–313.
2. Gohil, G.S., Binsu, V.V. and Shahi, V.K. (2006) *Journ. of Membrane Sci.*, **280(1−2)**, 210–218.
3. Sanchez, M.I., Mishima, H.T. and De Lopez, M.B.A. (1997) *J. Appl. Electrochem.*, **27**, 831−838.
4. Kuhn, H.H., Child, A.D. and Kimbrell, W.C. (1995) *Synth. Met.*, **71**, 2139−2142.
5. Lin, C.W., Hwang, B.J. and Lee, C.R. (1998) *Mater. Chem. Phys.*, **55**, 139−144.
6. Selampinar, E., Toppare, L., Akbulut, U., Yalçın, T. and Suzer, S. (1995) *Synth. Met.*, **68**, 109−116.
7. Whittal, I.R., Mcdonagh, A.M. and Humphrey, M.G. (1998) *Adv. Organomet. Chem.*, **42**, 291−362.
8. Grenier, A., Bolle, B., Hesemann, P., Obeski, J.M. and Sander, R. (1996) *Macromol. Chem. Phys.*, **197**, 113−134.
9. Sen, S., Gülce, A. and Gülce, H. (2004) *Biosensors and Bioelectronics*, **19**, 1261−1268.
10. Miller, J.S., Epstein, A.J. and Reiff, W.M. (1996) *Chem. Rev.*, **88**, 201−220.
11. Dodabalapur, A., Torsi, L. and Katz, H.E. (1995) *Science*, **268**, 270−271.
12. Al-Ahmed, A., Mohammed, F. and Rahman, M.Z.A. (2006) *Journ. of Appl. Polym. Sci.*, **99**, 437−448.
13. Ballav, N. (2005) *Mat. Sci. and Eng. B.*, **123**, 115−122.
14. Rubio Retama, J., Mecerreyes, D., Lopez-Ruiz, B. and Lopez-Cabarcos, E. (2005) *Colloids and Surfaces A: Physicochem. Eng. Aspects.*, **270**, 239−244.
15. Kurosawa, S., Teja, A.S., Kowalik, J. and Tolbert, L. (2006) *Synthetic Metals*, **156**, 146−153.
16. DePaoli, M., Panero, S., Prosperi, P. and Scrosati, B. (1990) *Electrochim. Acta.*, **35**, 1145.
17. DePaoli, M.A., Waltman, R.J., Diaz, A.F. and Bargon, J. (1984) *J. Chem. Soc. Chem. Commun.*, , 1015−1016.
18. Lindsey, S.L. and Street, G.B. (1984) *Synth. Metals*, **65**, 67−69.
19. Chiu, H.T., Lin, J.S. and Huang, C.M. (1992) *J. Appl. Electrochem.*, **222**, 358−363.
20. Wang, H.L., Toppare, L. and Fernandez, J.E. (1990) *Macromolecules*, **23**, 1053−1059.
21. Migahed, M.D., Ishra, M., Fahmy, T. and Barakat, A. (2004) *Journ. of Physics and Chem. of Solids.*, **65**, 1121−1125.

22. Gülce, H., Özyörük, H. and Yıldız, A. (1994) *Ber Bunsenges Phys. Chem.*, **98**, 228.

23. Gülce, H., Özyörük, H. and Yıldız, A. (1995) *Electroanalysis*, **7**, 178–183.

24. Smith, T.W., Kuder, J.E. and Wychick, D. (1976) *J. Polym. Sci.*, **14**, 2433–2448.

25. Maia, G., Ticianelli, E.A. and Nart, F.C. (1994) *Zeitschrift Phys. Chem.*, **186**, 245.

26. Menon, V., Lei, J. and Martin, C. (1996) *Chem. Mater.*, **8**, 2382–2390.

27. Tian, B. and Zerbi, G. (1990) *J. Chem. Phys.*, **92**, 3892–3898.

28. Bittihn, R., Ely, G. and Woeffler, F. (1987) *Makromol. Chem. Macromol. Symp.*, **8**, 51–59.

29. Cakmak, G., Küçükyavuz, Z. and Küçükyavuz, Ş. (2005) *Synthetic Metals*, **151**, 10–18.

30. Zuo, F., Angelopoulos, M., MacDiarmid, A.G. and Epstein, A. (1987) *J. Phys. Rev. B.*, **36**, 3475–3478.

31. Kobayashi, A., Ishikawa, H., Amano, K., Satoh, M. and Hasegawa, E. (1993) *J. Appl. Phys.*, **74(1)**, 296–299.

32. Han, M.G. and Im, S.S. (2000) *Polymer*, **41**, 3253–3262.

33. Road, A. *Magnetic Susceptibility Balance*; Instruction Manual; Christian Scientific Equipment Ltd: East Gateshead Industrial Estate, U.K. No. 6232, p8, 1993.

34. Gupta, M.C. and Sindhimeshram, D.C. (1994) *Ind. J. Chem., Sect A.*, **33**, 558.